

Explicit Adaptive Symplectic Integrators for solving Hamiltonian Systems

Sergio Blanes · Arieh Iserles

Received: date / Accepted: date

Abstract We consider Sundman and Poincaré transformations for the long-time numerical integration of Hamiltonian systems whose evolution occurs at different time scales. The transformed systems are numerically integrated using explicit symplectic methods. The schemes we consider are explicit symplectic methods with adaptive time steps and they generalise other methods from the literature, while exhibiting a high performance. The Sundman transformation can also be used on non-Hamiltonian systems while the Poincaré transformation can be used, in some cases, with more efficient symplectic integrators. The performance of both transformations with different symplectic methods is analysed on several numerical examples.

Keywords Symplectic Integrators · Adaptive time step · Hamiltonian systems

1 Introduction

We consider the long-time numerical integration of dynamical systems whose evolution is governed by the Hamiltonian function

$$H = \frac{1}{2} \mathbf{p}^\top \mathbf{p} + V(\mathbf{q}), \quad (1)$$

SB acknowledges the support of the Ministerio de Ciencia e Innovación (Spain) under the coordinated project MTM2010-18246-C03 (co-financed by the ERDF of the European Union).

Sergio Blanes
Instituto de Matemática Multidisciplinar,
Universitat Politècnica de Valencia, E-46022 Valencia, Spain.
E-mail: serblaza@imm.upv.es

Arieh Iserles
DAMTP, Centre for Mathematical Sciences,
University of Cambridge, Wilberforce Rd,
Cambridge CB3 0WA, United Kingdom
E-mail: A.Iserles@damtp.cam.ac.uk

with $\mathbf{q}, \mathbf{p} \in \mathbb{R}^d$, and such that the system evolves at different time scales. Effective long-time numerical integration requires to use adaptive time steps, consequently we wish to implement symplectic methods with adaptive time steps. To this purpose, we consider both the Sundman and the Poincaré transformations. The schemes proposed generalise other methods from the literature and allow us to build new explicit adaptive symplectic schemes exhibiting a high performance.

Numerical solution of Hamiltonian systems is frequently carried out by symplectic integrators (SIs) due to their good performance in moderate and long-time integration Hairer et al (2006); Iserles (2008); Leimkuhler and Reich (2004); McLachlan and Quispel (2002); Sanz-Serna and Calvo (1994). SIs belong to the family of *Geometric Numerical Integrators* (methods which preserve important qualitative and geometric properties of the underlying differential system) and are arguably the most popular methods in this class. Certain qualitative properties of the evolution, like symplecticity, are preserved and, in general, they exhibit smaller error growth along the numerical trajectory.

Splitting methods applied to separable Hamiltonian systems are the most frequently used symplectic integrators. Denoting by Φ_t^H the t -flow of the system, $\mathbf{z}(t) = \Phi_t^H(\mathbf{z}(0))$, with $\mathbf{z} = (\mathbf{q}, \mathbf{p})^\top$, the exact flow for one time step, h , can be approximated by a composition of the flows associated to the kinetic energy $\Phi_h^{[T]}$ and potential energy, $\Phi_h^{[V]}$. The second order *VTV* leap-frog/Störmer/Verlet method is given by the composition

$$\Psi_h \equiv \Phi_{h/2}^{[V]} \circ \Phi_h^{[T]} \circ \Phi_{h/2}^{[V]} \quad : \quad \begin{cases} \mathbf{p}_{n+1/2} = \mathbf{p}_n - \frac{h}{2} \nabla_{\mathbf{q}} V(\mathbf{q}_n) \\ \mathbf{q}_{n+1} = \mathbf{q}_n + h \mathbf{p}_{n+1/2} \\ \mathbf{p}_{n+1} = \mathbf{p}_{n+1/2} - \frac{h}{2} \nabla_{\mathbf{q}} V(\mathbf{q}_{n+1}) \end{cases} . \quad (2)$$

(Analogously, one can also take the *TVT* version.)

More accurate results can be obtained by using higher order methods. Splitting symplectic methods exist for a range of problems with different structure, leading to high-performance numerical schemes. For instance, splitting Runge–Kutta–Nyström (RKN) methods are tailored for Hamiltonian systems with quadratic kinetic energy, and there are also splitting methods tailored for perturbed systems where the Hamiltonian takes the form

$$H = H_0(\mathbf{p}, \mathbf{q}) + \varepsilon H_I(\mathbf{q}) = \left(\frac{1}{2} \mathbf{p}^\top \mathbf{p} + V_0(\mathbf{q}) \right) + \varepsilon V_I(\mathbf{q}), \quad (3)$$

where H_0 is exactly solvable and $0 < |\varepsilon| \ll 1$, an important such case being perturbed Kepler problems. We can then adapt the Verlet method (2) to the composition

$$\Psi_h^{[2]} \equiv \Phi_{h/2}^{[H_I]} \circ \Phi_h^{[H_0]} \circ \Phi_{h/2}^{[H_I]} = \Phi_h^H + \mathcal{O}(\varepsilon h^3) \quad (4)$$

to gain a factor ε in the accuracy Kinoshita et al (1991); Wisdom and Holman (1991).

A systematic procedure to build higher-order methods was introduced in Creutz and Gocksch (1989); Suzuki (1990); Yoshida (1990), and since then considerable effort has been expanded in order to construct new symplectic integrators with smaller local errors at a given computational cost. A significant number of new split symplectic integrators have been published for a wide number of problems

with different structures like RKN methods or methods for near-integrable systems (see Blanes et al (2008); Hairer et al (2006); Laskar and Robutel (2001); Leimkuhler and Reich (2004); McLachlan (1995a); McLachlan and Quispel (2002, 2006); Sanz-Serna and Calvo (1994) and references therein).

Unfortunately, the high performance of symplectic integrators is typically associated with the use of constant time steps. In contrast, adaptive variable time-step methods are often superior to fixed time-step methods when applied to problems with varying evolutionary time scales, since they lead to more regular problems with reduced local errors.

Once standard techniques for changing the time step are included in a symplectic integrator, several of the favourable properties of symplectic methods are lost Calvo and Sanz-Serna (1993); Gladman et al (1991); Skeel (1993). This procedure to change the time step does not destroy the symplectic structure but, roughly speaking, it can be considered as the exact solution of a perturbed time-dependent Hamiltonian, $H(\mathbf{q}, \mathbf{p}) + \delta\tilde{H}(\mathbf{q}, \mathbf{p}, t)$. (In the constant-step scenario \tilde{H} is independent of t .) Unless the time step is changed properly, secular error terms appear in the perturbed Hamiltonian and the errors in energy and position grow similarly to standard non-symplectic integrators: the advantages of symplecticity are thus lost.

Integrators with variable time step and non-secular error terms have been proposed in the literature. They consist of a regularisation of the time

$$\frac{dt}{d\tau} = g(\mathbf{q}, \mathbf{p}) \quad (5)$$

with g a positive-definite function, whereby one integrates with a constant time step in the fictive time, τ Blanes and Budd (2005); Bond and Leimkuhler (1998); Calvo et al (1998); Hairer (1997); Hairer and Söderlind (2005); Holder et al (2001); Huang and Leimkuhler (1997); Mikkola (1997); Mikkola and Aarseth (2002); Mikkola and Tanikawa (1999); Preto and Tremaine (1999). The Levi-Civita or Kustaanheimo–Stiefel regularizations for solving the Kepler problem consider of a time transformation of this kind, which is then combined with a canonical transformation, and they have been successfully used for many years in celestial mechanics Blanes and Budd (2004); Stiefel and Scheifel (1971).

We consider the Sundman and the Poincaré transformations in a general form which include most of the existing methods as particular cases and improve their performance for most problems. That performance – their accuracy and computational cost alike – depends on the choice of the regularisation function, g , as well as in the way the system is split for its numerical integration.

In section 2 we review the Sundman transformation and present new techniques to construct efficient explicit methods. In section 3 we review the Poincaré transformation and present new splitting methods to solve efficiently the evolution for perturbed Hamiltonian systems or with quadratic kinetic energy. In section 4 we present several numerical examples to illustrate how the new methods apply as well as to illustrate their relative performance.

2 Explicit adaptive SIs using the Sundman transformation

The Sundman transformation takes the real time as a new coordinate and introduces a fictitious time, τ in the following manner,

$$\frac{d}{d\tau} \begin{Bmatrix} \mathbf{q} \\ \mathbf{p} \\ t \end{Bmatrix} = \begin{Bmatrix} g(\mathbf{q}, \mathbf{p})\mathbf{p} \\ -g(\mathbf{q}, \mathbf{p})\nabla V(\mathbf{q}) \\ g(\mathbf{q}, \mathbf{p}) \end{Bmatrix}. \quad (6)$$

This equation loses the symplectic structure and, in addition, most explicit methods available in the literature for the numerical integration of the Hamiltonian (1) cannot be used or are highly inefficient in this setting. It has been shown, however, that if a reversible time-symmetric method is used, many good properties for long-time integrations are retained. Note that if the regularisation function g is frozen at each step (or at each stage inside a step) then we can use an explicit symplectic integrator and the coordinates (\mathbf{q}, \mathbf{p}) will evolve through a symplectic transformation. Thus, it is only necessary to look for an appropriate procedure to freeze the function g in a manner which renders the whole numerical integration reversible and time-symmetric, leading to an adaptive symplectic and time-reversible integrator.

We introduce an auxiliary scalar variable, z , and a positive-definite and invertible function, $G(z)$, such that $G(z) = g(\mathbf{z})$. To avoid some instabilities, we differentiate this equation so, the system to be solved is

$$\frac{d}{d\tau} \begin{Bmatrix} \mathbf{q} \\ \mathbf{p} \\ t \\ z \end{Bmatrix} = \begin{Bmatrix} G(z)\mathbf{p} \\ -G(z)\nabla V(\mathbf{q}) \\ G(z) \\ (G(g(\mathbf{q}, \mathbf{p}))^{-1})' G(z) (\nabla g(\mathbf{q}, \mathbf{p}) \cdot \mathbf{f}) \end{Bmatrix} \quad (7)$$

where $\mathbf{f} \equiv J\nabla H(\mathbf{q}, \mathbf{p})$ and J denotes the standard $(2d) \times (2d)$ symplectic matrix.

Numerical integration of this problem has been considered in the literature for different choices of the function $G(z)$, the monitor function, $g(\mathbf{q}, \mathbf{p})$ and by splitting the system in different ways. Since $G(z)/g(\mathbf{q}, \mathbf{p}) = 1$ is a first integral of the system, it has been usual to substitute $G(z)$ by $g(\mathbf{q}, \mathbf{p})$ in different places on the right-hand side of the equation, and in particular in the equation for $dz/d\tau$. For example, Huang and Leimkuhler (1997); Leimkuhler and Reich (2004) employs the choice $G(z) = z$ while Hairer and Söderlind (2005); Mikkola and Aarseth (2002) (see also (Hairer et al, 2006, Sec. VIII.3.2)) use $G(z) = 1/z$. These are two particular cases of the more general function $G(z) = z^\alpha$, where the choice $\alpha = 0$ corresponds to no regularisation. As we will see, the choice of $G(z)$ plays an important role in the performance of the algorithm.

The *monitor function* g is also very important in constructing efficient algorithms Blanes and Budd (2005). For the system (1), fast evolutions usually occur close to the singularities of the potential. Thus, it makes sense to consider a function depending only on the coordinates, say, $g(\mathbf{q})$. However, other choices are also valid and the main differences impacts on the complexity when computing the equation for z' (where the prime denotes the derivative with respect to τ).

Finally, one has to decide how to split the system in order to use a time-symmetric splitting method which preserves symplecticity for the coordinates \mathbf{q}, \mathbf{p} . For example, in Hairer and Söderlind (2005) (see also (Hairer et al, 2006, Sec.

VIII.3.2)), where $G(z) = 1/z$, $g(\mathbf{q}) = (\mathbf{q}^\top \mathbf{q})^\gamma$ (for problems where the singularity of the potential is at the origin), the function $G(z)$ is replaced by $g(\mathbf{q})$ in the equation of z' , and the system is split as follows

$$\frac{d}{d\tau} \begin{Bmatrix} \mathbf{q} \\ \mathbf{p} \\ t \\ z \end{Bmatrix} = \underbrace{\begin{Bmatrix} \frac{1}{z} \mathbf{p} \\ -\frac{1}{z} \nabla V(\mathbf{q}) \\ \frac{1}{z} \\ 0 \end{Bmatrix}}_{\mathbf{f}_A} + \underbrace{\begin{Bmatrix} \mathbf{0} \\ \mathbf{0} \\ 0 \\ -\gamma \frac{\mathbf{q}^\top \mathbf{p}}{\mathbf{q}^\top \mathbf{q}} \end{Bmatrix}}_{\mathbf{f}_B}. \quad (8)$$

The system is then solved using the composition

$$\Psi_h = \Phi_{h/2}^{(B)} \circ \Phi_h^{(A)} \circ \Phi_{h/2}^{(B)} \quad (9)$$

with $h \equiv \delta\tau$. Here, $\Phi_{h/2}^{(B)}$ is used only to change the time step for the real time. Consequently, one can replace $\Phi_h^{(A)}$ by the desired symplectic integrator to advance \mathbf{q} , \mathbf{p} and t . This is a second-order approximation in the auxiliary variable z , which is not relevant to the accuracy of the method. The practical order of accuracy follows from the order of the method used to approximate $\Phi_h^{(A)}$.

This is a simple time-reversible explicit symplectic integrator and it is perhaps the most efficient algorithm for low to moderate accuracies. However, if accurate results are desired, high-order methods are necessary. High-order methods usually require many evaluations per step and demonstrate their superior performance when relatively large time steps are used in lieu of the extra per-step cost. However, this scheme changes the time step only when the flow $\Phi_h^{(B)}$ is computed, hence to use a relatively large time step can be dangerous when the system moves close to the singularities because the scheme has no opportunity to adapt the time step.

We then propose to split the system as follows,

$$\frac{d}{d\tau} \begin{Bmatrix} \mathbf{q} \\ \mathbf{p} \\ t \\ z \end{Bmatrix} = \underbrace{\begin{Bmatrix} G(z) \mathbf{p} \\ \mathbf{0} \\ G(z) \\ 0 \end{Bmatrix}}_{\mathbf{f}_A} + \underbrace{\begin{Bmatrix} \mathbf{0} \\ \mathbf{0} \\ 0 \\ (G(g)^{-1})' G(z) (\nabla g \cdot \mathbf{f}) \end{Bmatrix}}_{\mathbf{f}_B} + \underbrace{\begin{Bmatrix} \mathbf{0} \\ -G(z) \nabla V \\ \mathbf{0} \\ 0 \end{Bmatrix}}_{\mathbf{f}_C}. \quad (10)$$

The right hand side of the equation for $dt/d\tau$ could be put into any of the three vector fields and each part would be still exactly solvable but it is advantageous to keep it in either \mathbf{f}_A or \mathbf{f}_C .

We propose to use the following symmetric second order composition

$$S_h^{[2]} = \Phi_{h/2}^{(A)} \circ \Phi_{h/2}^{(B)} \circ \Phi_h^{(C)} \circ \Phi_{h/2}^{(B)} \circ \Phi_{h/2}^{(A)}. \quad (11)$$

Other sequences of the maps are also valid. Next, to reach high accuracy one can use this method as the basic method to build higher order methods by composition, i.e.

$$S_h^{[2p]} = S_{\alpha_m h}^{[2]} \circ \dots \circ S_{\alpha_1 h}^{[2]}$$

where the coefficients α_i are chosen appropriately to build efficient methods of order $2p$ in the time step h Hairer et al (2006); McLachlan (1995b); McLachlan and Quispel (2002); Sophroniou and Spaletta (2005). Notice that in this approach the time step is adjusted along the internal stages of the method instead of adjusting the time step by the end of the step.

Constructing methods of order four or six, it is usually more efficient to consider a composition of a first order method, say, $\Phi_h = \Phi_h^{(A)} \circ \Phi_h^{(B)} \circ \Phi_h^{(C)}$ and its adjoint $\Phi_h^* = \Phi_h^{(C)} \circ \Phi_h^{(B)} \circ \Phi_h^{(A)}$ in an appropriate sequence Blanes and Moan (2002).

The choice of the monitor function We have to remark that the choice of the monitor function g is essential in constructing efficient methods Blanes and Budd (2005); Budd et al (2001); Calvo et al (1998); Hairer (1997); Hairer et al (2006). The numerical accuracy of a given scheme can be similar for different choices of g while its computational cost can change drastically. Then, one has to choose the most appropriate monitor function which must also satisfy the required conditions (e.g. preserving scaling invariance of the system or any reversing symmetry) and this has to be done in tandem with the choice of the function $G(z)$ in order to obtain simple and easy to compute expression for z' . For example, if the potential function is given by $V(r)$ with $r = (\mathbf{q}^\top \mathbf{q})^{1/2}$ then it seems appropriate to choose $g = g(r)$ because then, replacing $G(z)$ by $g(r)$, the equation for z' becomes $z' = F(r)(\mathbf{q}^\top \mathbf{p})$, with $F(r)$ a given scalar function. Another important property to be analysed is how the choice of the function $G(z)$ affects the performance of the numerical methods.

To sum up, the Sundman transformation allows us to build explicit time reversible adaptive integrators to high order. However, RKN methods or methods tailored for near integrable systems can not be used, unless the system is split as in (8), which has some limitations as previously mentioned. To circumvent this problem, we will consider the Poincaré transformation.

2.1 Some other particular cases

The scheme that we have proposed generalises other schemes used to numerically solve the system (6) which have appeared in the literature.

In Leimkuhler and Reich (2004) an algorithm (previously obtained in Huang and Leimkuhler (1997)) is presented which corresponds to $G(z) = z$, considering $z = g$ in the equation of z' , and employing the splitting

$$\frac{d}{d\tau} \begin{pmatrix} \mathbf{q} \\ \mathbf{p} \\ t \\ z \end{pmatrix} = \underbrace{\begin{pmatrix} z\mathbf{p} \\ \mathbf{0} \\ z \\ 0 \end{pmatrix}}_{\mathbf{f}_A} + \underbrace{\begin{pmatrix} \mathbf{0} \\ -z\nabla V \\ 0 \\ g(\nabla g \cdot \mathbf{f}) \end{pmatrix}}_{\mathbf{f}_B} \quad (12)$$

where we let $g(\mathbf{q}, \mathbf{p}) = \|\mathbf{f}\|$. With this splitting and the choice of g , the final algorithm has to be necessarily implicit. In Leimkuhler and Reich (2004) the h -flow Φ_h^B is approximated by the first order explicit Euler method, $\tilde{\Phi}_h^B$, and its

implicit adjoint method, $\tilde{\Phi}_h^{*B}$, and constructs the following implicit symmetric second order method

$$S_h = \tilde{\Phi}_{h/2}^B \circ \Phi_h^A \circ \tilde{\Phi}_{h/2}^{*B}. \quad (13)$$

This method requires the computation of the Hessian of the potential and for this reason it can be computationally costly for many problems.

In Mikkola and Aarseth (2002), the authors consider a monitor function depending only on the coordinates, $g(\mathbf{q})$, let $G(z) = 1/z$ (although the method is presented in terms of the function $\Omega(\mathbf{q}) = 1/g(\mathbf{q})$) so that $z' = -(\nabla_{\mathbf{q}}g \cdot \mathbf{p})/g$ and the algorithm proposed is basically equivalent to considering the splitting

$$\frac{d}{d\tau} \begin{Bmatrix} \mathbf{q} \\ \mathbf{p} \\ t \\ z \end{Bmatrix} = \underbrace{\begin{Bmatrix} \frac{1}{z}\mathbf{p} \\ z\mathbf{0} \\ \frac{1}{z} \\ z\mathbf{0} \end{Bmatrix}}_{\mathbf{f}_A} + \underbrace{\begin{Bmatrix} \mathbf{0} \\ -g\nabla V \\ 0 \\ -\frac{1}{g}(\nabla_{\mathbf{q}}g \cdot \mathbf{p}) \end{Bmatrix}}_{\mathbf{f}_B}. \quad (14)$$

Note that the equation for \mathbf{f}_B is exactly solvable because the equation for z' is linear in \mathbf{p} . With this splitting, in Mikkola and Aarseth (2002) the authors construct the scheme

$$S_h = \Phi_{h/2}^A \circ \Phi_h^B \circ \Phi_{h/2}^A \quad (15)$$

which is then taken as the basic method to be used with the Gragg–Bulirsch–Stoer extrapolation method. However, an extrapolation method based on a symmetric second order symplectic integrator is not appropriate because it loses symplecticity and its benefits for long-time integration. One can obtain, however, pseudo-symplectic integrators by extrapolation if the basic method is of higher order Blanes et al (1999); Chan and Murua (2000) and qualitative properties are preserved up to higher order than the order of the method. We recommend his procedure only when high accuracy is desired, say, to nearly round-off level and relatively short time integrations.

Alternatively, one can solve the system (14) by standard splitting methods for separable systems. Here, both \mathbf{q} and \mathbf{p} evolve through symplectic maps only if $g\nabla V$ is the gradient of a potential, and this deserves further investigation.

3 The Poincaré transformation

Given a Hamiltonian $H(\mathbf{q}, \mathbf{p})$, the Poincaré transformation introduces the following new Hamiltonian in the extended phase space,

$$\bar{H}(\mathbf{q}, \mathbf{p}, q^t, p^t) = g(\mathbf{q}, \mathbf{p})(H(\mathbf{q}, \mathbf{p}) + p^t) \quad (16)$$

where $q^t \equiv t$ and p^t is its conjugate momentum. Note that H is autonomous, therefore \bar{H} does not depend on q^t , and p^t is a constant of motion whose value is usually taken as $p^t = -H_0$ with $H_0 \equiv H(\mathbf{q}(0), \mathbf{p}(0))$, consequently $\bar{H} = 0$ along the solution. The structure of the Hamiltonian \bar{H} differs in general from the structure of H , i.e. if H is separable in solvable parts, in general, \bar{H} will not be separable in solvable parts.

The Poincaré transformation applied to (1) corresponds to solving the evolution for the Hamiltonian (16), which we split

$$\bar{H}(\mathbf{q}, \mathbf{p}, q^t, p^t) = g(\mathbf{q}, \mathbf{p}) \left(\frac{1}{2} \mathbf{p}^\top \mathbf{p} + p^t \right) + g(\mathbf{q}, \mathbf{p}) V(\mathbf{q}). \quad (17)$$

Taking the monitor function

$$g(\mathbf{q}, \mathbf{p}) = \left(\frac{1}{2} \mathbf{p}^\top \mathbf{p} + p^t \right)^{\gamma-1}$$

and considering $\frac{1}{2} \mathbf{p}^\top \mathbf{p} + p^t = -V(\mathbf{q})$, the Hamiltonian being solved becomes separable,

$$\bar{H}(\mathbf{q}, \mathbf{p}, q^t, p^t) = \left(\frac{1}{2} \mathbf{p}^\top \mathbf{p} + p^t \right)^\gamma - (-V(\mathbf{q}))^\gamma. \quad (18)$$

This is equivalent to the Hamiltonian used in Preto and Tremaine (1999), where it was taken with the monitor function

$$g = \frac{f(\frac{1}{2} \mathbf{p}^\top \mathbf{p} + p^t) - f(-V(\mathbf{q}))}{H(\mathbf{q}, \mathbf{p}) + p^t} \quad (19)$$

and it was assumed that $f(u) = u^\gamma$ for some $\gamma \neq 0$. The particular case $f(u) = \log u$ was previously considered in Mikkola (1997); Mikkola and Tanikawa (1999). $f(u)$ must be an analytic function, where the apparent singularity at $H = -p^t$ is removable: take the Taylor series of f about the point $-V(\mathbf{q})$ and use $\frac{1}{2} \mathbf{p}^\top \mathbf{p} + p^t = H(\mathbf{q}, \mathbf{p}) + p^t - V(\mathbf{q})$. Since numerically $\frac{1}{2} \mathbf{p}^\top \mathbf{p} + p^t \simeq -V(\mathbf{q})$, we have $g \simeq f'(-V(\mathbf{q}))$, where $f(u)$ must be a function such that $f'(u) > 0$, with no singularities in the domain of interest. The system is still separable, but it is no longer quadratic in the kinetic energy and RKN methods cannot be used.

In practice, we have observed in some numerical examples that $\frac{1}{2} \mathbf{p}^\top \mathbf{p} + p^t$ (or $-V(\mathbf{q})$) can be negative along the trajectory and the algorithm breaks down. We can circumvent this problem if we consider instead the splitting

$$\bar{H}(\mathbf{q}, \mathbf{p}, q^t, p^t) = \left(\frac{1}{2} \mathbf{p}^\top \mathbf{p} \right)^\gamma - (-V(\mathbf{q}) - p^t)^\gamma. \quad (20)$$

Separable Hamiltonian with kinetic energy quadratic in momenta If we consider the Hamiltonian (1) and a monitor function depending only on the coordinates, $g(\mathbf{q})$, the Poincaré transformation leads to the following enlarged Hamiltonian system which we split as follows

$$\bar{H} = K_1(\mathbf{q}, \mathbf{p}) + K_2(\mathbf{q}, p^t) = \frac{1}{2} g(\mathbf{q}) \mathbf{p}^\top \mathbf{p} + g(\mathbf{q}) (V(\mathbf{q}) + p^t). \quad (21)$$

Now, $K_2(\mathbf{q}, p^t)$ is exactly solvable and $K_1(\mathbf{q}, \mathbf{p})$ is, in general, not solvable but it is a product of solvable parts. On the other hand, it is important to notice that K_1 is quadratic in momenta. If $\{K_1, K_2\}$ denotes the Poisson bracket of the functions K_1, K_2 , it is easy to see that $\{K_2, \{K_2, \{K_2, K_1\}\}\} = 0$, displaying an algebraic structure similar to Nyström problems. Thus, symplectic splitting Nyström methods can be used, and this is usually more accurate and stable for these problems than general symplectic integrators.

For this purpose, we need an algorithm to approximate efficiently and accurately the evolution for the Hamiltonian

$$K_1 = \frac{1}{2}g(\mathbf{q})\mathbf{p}^\top \mathbf{p}.$$

In Blanes and Budd (2005) it is shown that in some cases one can find a canonical transformation, $(\mathbf{q}, \mathbf{p}) \rightarrow (\mathbf{Q}, \mathbf{P})$ where $\mathbf{q} = \Phi(\mathbf{Q})$, $\Phi'(\mathbf{Q})^\top \mathbf{p} = \mathbf{q}$, such that K_1 depends only on the new momenta. Unfortunately, this occurs rarely and we look for an alternative procedure. This can be done in different ways, and the most appropriate one will depend on the particular problem. If $g(\mathbf{q})$ is cheap to compute function e.g. the singularity of the potential involves only few contributions (i.e. if it involves only two bodies in a N -body problem) we can numerically solve efficiently the equations for K_1 to roundoff accuracy at each stage.

For instance, we can use a logarithmic method. Notice that the evolution for one time step $\Delta\tau$ of $K_1 = \frac{1}{2}g(\mathbf{q})\mathbf{p}^\top \mathbf{p}$ is equivalent to the evolution for one time step $\Delta\delta = E_1\Delta\tau$ with $E_1 = K_1$ of the Hamiltonian

$$K_L = K_{L,1} + K_{L,2} = \log(g(\mathbf{q})) + \log(\mathbf{p}^\top \mathbf{p}), \quad (22)$$

(during this evolution K_1 is kept constant) as is immediate to see from the Hamiltonian equations. At near collisions, $\frac{1}{2}\mathbf{p}^\top \mathbf{p}$ and g take large and small values, respectively, but logarithmic functions reduce these large values and maintain the effectiveness of the splitting. The Hamilton equations for $K_{L,1}$ and $K_{L,2}$ are:

$$\begin{cases} \frac{d\mathbf{q}}{d\tau} = 0, \\ \frac{d\mathbf{p}}{d\tau} = -\frac{1}{g}\nabla_{\mathbf{q}}g, \end{cases} \quad \begin{cases} \frac{d\mathbf{q}}{d\tau} = 2\frac{\mathbf{p}}{\mathbf{p}^\top \mathbf{p}}, \\ \frac{d\mathbf{p}}{d\tau} = 0. \end{cases} \quad (23)$$

In general, we can take g in a very simple form, just by considering the singularities of the potential. If the system is scaling invariant (or close to it) as happens for most practical potentials with singularities or strong interactions, the optimal regularisation function g is closely related with the choice which preserves this scaling invariance Blanes and Budd (2004, 2005); Budd et al (2001). Then, if we take

$$g = (\mathbf{q}^\top \mathbf{q})^{\gamma/2} \quad (24)$$

for an appropriate choice of γ , we have

$$\frac{1}{g}\nabla_{\mathbf{q}}g = \gamma\frac{\mathbf{q}}{\mathbf{q}^\top \mathbf{q}}$$

rendering both parts of (23) trivial to compute with simple and cheap arithmetic operations, so the evolution for K_1 can be easily computed to roundoff accuracy with marginal extra cost.

It is important to bear in mind that, solving K in (22), the value of E_1 changes from one stage to the next for the entire method. As we have already mentioned, to change the Hamiltonian at each step from information originating in the previous step introduces, in general, secular errors. To diminish these errors to nearly roundoff, the system has to be numerically solved to a very high accuracy, so these errors can be sufficiently diminished for practical purposes. This can be achieved, e.g. using a high order composition.

A nearly-integrable Hamiltonian Let us now consider the perturbed Hamiltonian

$$H(\mathbf{q}, \mathbf{p}) = H_0(\mathbf{q}, \mathbf{p}) + \varepsilon H_1(\mathbf{q}), \quad (25)$$

where H_0 is exactly solvable and $0 < |\varepsilon| \ll 1$, but occasionally the perturbation can approach a singularity and it can take large values. For this problem it is convenient to split the Hamiltonian into the dominant part and the perturbation because the error of numerical methods reduces considerably, but we need to adapt the time step when the perturbation is more relevant. This is the case, for instance, with the N -body problem in the solar system, where the Hamiltonian can be split into pure Kepler problems and weak interactions between planets. In some cases, however, close approaches between the planets or asteroids can occur and, in spite of ε being a small parameter, the Hamiltonian $H_1(\mathbf{q})$ can be nearly singular. In this case it is convenient to introduce adaptivity.

There are two natural choices for the regularisation function: $g(H_0 + p^t)$ and $g(\mathbf{q})$. In the first case, the Hamiltonian to solve is (considering that $H_0 + p^t = -\varepsilon H_1$)

$$\bar{H} = g(H_0 + p^t)(H_0 + p^t) + \varepsilon g(-\varepsilon H_1)H_1. \quad (26)$$

The Hamiltonian $g(H_0 + p^t)(H_0 + p^t)$ exhibits the same difficulty as H_0 , and it is also exactly solvable. However, for the choice $g(u)u = u^\gamma$ we have found in several problems that $H_0 + p^t$ takes negative values. In that case, one can integrate, backward in time, the Hamiltonian, $-H$, in order to keep both parts positive.

The evolution of a Hamiltonian system is unaltered by adding an arbitrary constant so, we can introduce a constant δ such that

$$\varepsilon H_1 + \delta < 0,$$

consequently $H_0 + p^t > 0$, and the new Hamiltonian to consider is

$$\bar{H} = g(H_0 + p^t)(H_0 + p^t) - g(-\varepsilon H_1 - \delta)(-\varepsilon H_1 - \delta), \quad (27)$$

which has lost the structure of a perturbed system: the performance of the splitting methods tailored for perturbed systems is then seriously degraded.

However, if we take e.g. $g(\mathbf{q}) = (\mathbf{q}^\top \mathbf{q})^\gamma$, the Hamiltonian becomes

$$\bar{H} = (\mathbf{q}^\top \mathbf{q})^\gamma (H_0 + p^t) + \varepsilon (\mathbf{q}^\top \mathbf{q})^\gamma H_1(\mathbf{q}), \quad (28)$$

which retains the near integrable structure, but we need to solve accurately and efficiently the Hamiltonian

$$K_1 = (\mathbf{q}^\top \mathbf{q})^\gamma (H_0 + p^t). \quad (29)$$

We can use the logarithmic method as previously, the main trouble being that $H_0 + p^t$ must be positive definite (if not, we can take $K_1 = -(\mathbf{q}^\top \mathbf{q})^\gamma (-H_0 - p^t)$ and integrate backward in time the Hamiltonian $(\mathbf{q}^\top \mathbf{q})^\gamma (-H_0 - p^t)$) and each stage would need to evaluate the Hamiltonian H_0 several times. If this part is not computationally costly and the perturbation H_1 is the most costly part of the algorithm, this splitting might be useful because it benefits from the perturbed structure. We conclude with an interesting open problem, efficient time-reversible SIs for Hamiltonians of the form $H = H_1(\mathbf{q}, \mathbf{p})H_2(\mathbf{q}, \mathbf{p})$, where H_1 and H_2 are exactly solvable Hamiltonian functions.

4 Numerical Examples

We consider the integration of several examples by considering both the Sundman and the Poincaré transformations jointly with appropriate splitting and composition methods. Given a symmetric second order (implicit or explicit) method, $S_h^{[2]}$, we consider m -stage symmetric compositions of order n as follows

$$S_m n \equiv S_{\alpha_1 h}^{[2]} \circ S_{\alpha_2 h}^{[2]} \cdots S_{\alpha_k h}^{[2]} \circ S_{\alpha_{k+1} h}^{[2]} \circ S_{\alpha_k h}^{[2]} \cdots S_{\alpha_2 h}^{[2]} \circ S_{\alpha_1 h}^{[2]}$$

with $m = 2k + 1$. The following composition methods are chosen for that purpose

- $S_5 4$: the 5-stage fourth-order composition,
- $S_9 6$: the 9-stage sixth-order composition,
- $S_{17} 8$: the 17-stage eighth-order composition,

and whose coefficients can be found in Hairer et al (2006). In Sophroniou and Spaletta (2005) more elaborated compositions with additional extra stages are obtained with slightly improved performance.

The following splitting methods are considered for problems where RKN methods or methods for near-integrable systems can be used

- $RKN_6 4$: the 6-stage fourth-order BAB method from Blanes and Moan (2002),
- $RKN_{11} 6$: the 11-stage sixth-order BAB method from Blanes and Moan (2002),
- $M84$: the 5-stage (8,4) BAB method from McLachlan (1995a) for perturbed systems.

4.1 The one-dimensional Kepler problem

Let us consider the Kepler problem, which possesses periodic orbits with close approaches. Such an orbit has a radial coordinate q with associated momentum p which evolves according to the Hamiltonian

$$H = \frac{1}{2} p^2 - \frac{1}{q} + \frac{\varepsilon}{q^2}, \quad (30)$$

where $\sqrt{\varepsilon}$ is the angular momentum. In numerical tests we take the initial conditions $(q_0, p_0) = (1, 0)$ and $\varepsilon = 0.001$ (which allows for very close approaches).

We first study the performance of different algorithms when using the Sundman transformation. We take $G(z) = 1/z$, integrate until $t = 100$ and measure the average relative error in energy when considering the splitting shown in (8)–(9) or when considering (10)–(11). In the first case, The compositions are used to approximate $\Phi_h^{(A)}$ in (9) as composition of the leapfrog scheme as the basic method, or they are used as compositions of the second-order scheme (11). The time step is adjusted in all cases such that the final time is reached using approximately 50000 evaluations of the potential. Fig. 1 displays the results obtained when considering the regularisation function $g = q^\gamma$ for different values of γ . It is clear from the results that adjusting the time step through the variable z along the internal stages of the method allows us to greatly improve the performance of the methods once high-order methods are used to reach high accuracy.

We next repeat the experiment for $G(z) = z^\alpha$ and different values of α . We measure the accuracy of $S_{17} 8$ when the monitor function $g = q^\gamma$ is used with its

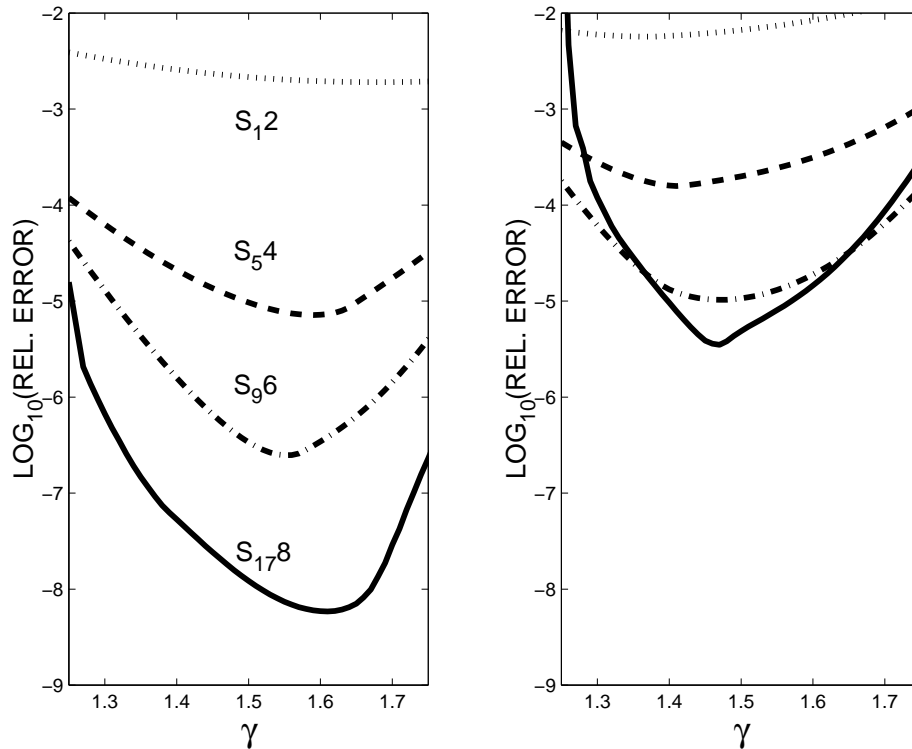


Fig. 1 Average error in energy for the numerical integration of the Hamiltonian (30) using the Sundman transformation with the splitting from (10)-(11) (left panel) or when considering (8)-(9) (right panel). The following methods are compared: the leap-frog S_{12} (dotted lines), S_{54} (dashed lines), S_{96} (dotted-dashed lines) and S_{178} (solid lines).

optimal value $\gamma = 1.6$ and the most accurate splitting (10)–(11). Figure 2 shows the results obtained when solving the equation for z' in two different ways:

$$z' = \left(\frac{\gamma}{\alpha} q^{\gamma/\alpha-1} p \right) z^\alpha \quad (31)$$

where q, p are taken constants along its integration which has exact solution (broken lines) or, once we replace z^α by q^γ ,

$$z' = \frac{\gamma}{\alpha} q^{\gamma+\gamma/\alpha-1} p \quad (32)$$

(solid lines). We observe that the two choices lead to considerably different results and it is clear that the choice of the function $G(z)$ can be relevant to the performance of the methods. The usual choice $G = 1/z$ is very close to optimal if one considers $z = 1/q^\gamma$ (it corresponds to taking $\alpha = -1$ in (32)) as it has been frequently done in the literature, and it is clearly better than the choice $z = q^\gamma$ (i.e. to take $\alpha = 1$ in (32)). We have repeated the numerical experiments for the more general one-dimensional potential, $V = 1/r^\beta - \varepsilon/r^{2\beta}$, for different choices of β and ε and the choice $G = 1/z$ was always very close to optimal one.

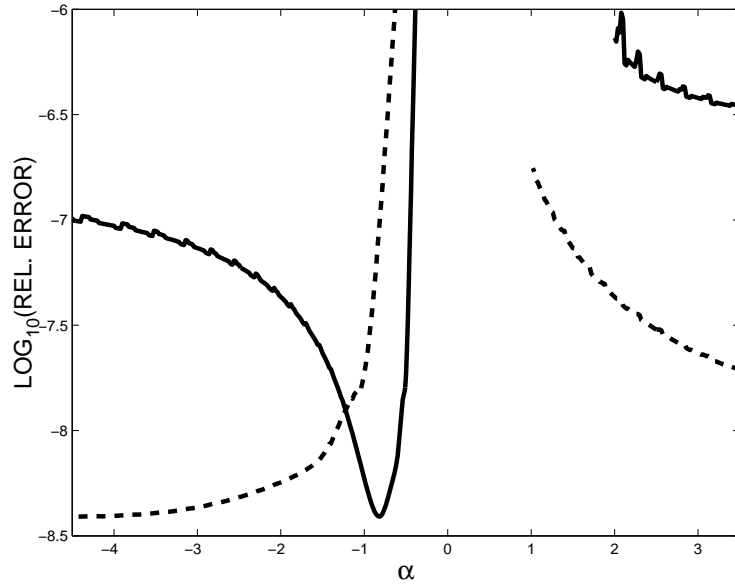


Fig. 2 Same as Fig. 1 for $g = q^\gamma$ and $\gamma = 1.6$ when considering the splitting shown in (10)-(11) and the eighth-order method S_{178} . We take $G(z) = z^\alpha$ for different values of α . Solid lines show the results when the equation (31) is used and broken lines show the results when the equation (32) is used.

Let us now integrate the system using the Poincaré transformation and the regularisation function $g = q^\gamma$. In that case (21) takes the form

$$K = T(q, p) + V(q, q^t) = \frac{1}{2}q^\gamma p^2 + q^\gamma \left(-\frac{1}{q} + \frac{\varepsilon}{q^2} + p^t \right). \quad (33)$$

We take the same initial conditions (so, $p^t = -(\frac{1}{2}p_0^2 - \frac{1}{q_0} + \frac{\varepsilon}{q_0^2}) = 1 - \varepsilon$) and $\gamma = 1.35$, which is roughly the optimal value for this type of methods Blanes and Budd (2005), and integrate until $t = 1000$. We integrate this system using the method RKN_{116} as follows

$$\Phi_h^{[6]} = \prod_{i=1}^{12} \Phi_{a_i h}^{[T, n]} \circ \Phi_{b_i h}^{[V]} \quad (34)$$

where $a_{12} = 0$ and the last map in one step is reused in the following step (in practice, the cost corresponds to 11 stages), and where

$$\Phi_{b_i h}^{[V]} : \begin{cases} q_{n+1} = q_n, \\ p_{n+1} = p_n - b_i h V'_q, \\ t_{n+1} = t_n + b_i h q^\gamma. \end{cases} \quad (35)$$

We compare its performance versus the S_{96} and S_{178} schemes which use the following generalization of the leapfrog method,

$$\Phi_h^{[2]} = \Phi_{h/2}^{[V]} \circ \Phi_h^{[T, n]} \circ \Phi_{h/2}^{[V]} \quad (36)$$

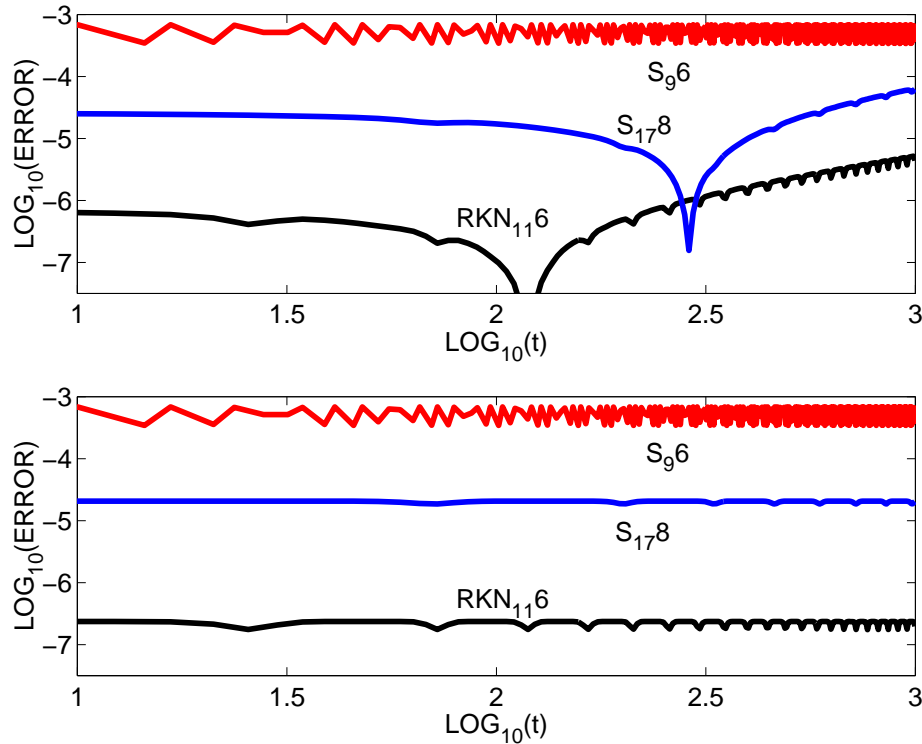


Fig. 3 Error in energy (averaged every 100 steps) for different methods and using all of them approximately the same number of evaluations. The logarithmic Hamiltonian is solved using the S_{96} method (top figure) and the S_{178} method (bottom figure).

as the basic method to build the higher order ones. In both cases, $\Phi_h^{[T,n]}$ denotes a n th-order approximation to the evolution associated to $T(q,p)$. Here, $T(q,p)$ is a product of a small and a large term near the collision. This evolution is approximated using the splitting of symmetric and symplectic integrators of order n for the logarithmic Hamiltonian

$$\bar{H} = \gamma \log(q) + 2 \log(p) \quad (37)$$

with a time step $E_1 h$. The exact solution is equivalent to the evolution associated to $T(q,p)$. We use S_{96} and S_{178} with the leapfrog as the basic method to approximate $\Phi_h^{[T,n]}$.

Fig. 3 exhibits the error in energy (the average error every 100 steps because the error oscillates). Each method is used with the fictive time step $\delta\tau = \frac{40}{9 \times 11 \times 17} m$, where m is the number of stages of each method, hence all methods need approximately the same number of evaluations to reach the final real time. In the top figure we show the results when the logarithmic Hamiltonian is solved using the S_{96} method. After some time, a linear error growth in energy is observed. We repeated the experiments but solving the logarithmic Hamiltonian with the S_{178} method (bottom figure) and the error growth has disappeared in the interval of interest. This scheme can be considered as a pseudo-symplectic integrator (a method

which preserves simplecticity at a higher order than the order of the method) and it is clear how important it is to solve this part accurately.

We have observed a good behaviour in the numerical experiments for long-time integration as well as the good performance of the RKN methods for problems with quadratic kinetic energy, and for this reason it makes good sense to consider this technique for other families of problems.

4.2 A perturbed Kepler problem

We consider in this subsection the two-dimensional perturbed Kepler problem

$$H = \frac{1}{2}(p_1^2 + p_2^2) - \frac{1}{r} + \frac{\varepsilon}{r^3}, \quad (38)$$

$r = \sqrt{q_1^2 + q_2^2}$, which *inter alia* describes in first approximation the dynamics of a satellite moving into the gravitational field produced by a slightly oblate planet. We take as initial conditions $q_1 = 1 - e$, $q_2 = 0$, $p_1 = 0$, $p_2 = \sqrt{(1+e)/(1-e)}$ which, for the unperturbed problem, would correspond to an orbit of period 2π , eccentricity e and energy $-\frac{1}{2}$. We integrate until the final real time $t = 1000$ for $e = 0.8$, $\varepsilon = 10^{-3}$ and measure the average relative error in energy versus the number of force evaluations for different choices of fictitious time steps.

We compare the performance of the methods when using the Sundman and the Poincaré transformation. For this problem we take the monitor function $g = r^\gamma$ for $\gamma = \frac{3}{2}$, which is close to optimal in both cases.

In the Sundman transformation we take $G(z) = 1/z$ and the splitting

$$\frac{d}{d\tau} \begin{Bmatrix} \mathbf{q} \\ \mathbf{p} \\ t \\ z \end{Bmatrix} = \underbrace{\begin{Bmatrix} \frac{1}{z}\mathbf{p} \\ \mathbf{0} \\ 0 \\ 0 \end{Bmatrix}}_{\mathbf{f}_A} + \underbrace{\begin{Bmatrix} \mathbf{0} \\ \mathbf{0} \\ 0 \\ -\gamma \frac{\mathbf{q}^\top \mathbf{p}}{\mathbf{q}^\top \mathbf{q}} \end{Bmatrix}}_{\mathbf{f}_B} + \underbrace{\begin{Bmatrix} \mathbf{0} \\ -\frac{1}{z}\nabla V(\mathbf{q}) \\ \frac{1}{z} \\ 0 \end{Bmatrix}}_{\mathbf{f}_C} \quad (39)$$

and we consider the S_{96} and the S_{178} methods as a composition of the symmetric second order (11).

Next, we consider the Poincaré transformation

$$\bar{H} = r^\gamma \frac{1}{2}(p_1^2 + p_2^2) + r^\gamma \left(-\frac{1}{r} + \frac{\varepsilon}{r^3} + p^t \right). \quad (40)$$

We integrate the Hamiltonian $r^\gamma \frac{1}{2}(p_1^2 + p_2^2)$ through the integration of the logarithmic Hamiltonian

$$K = \frac{\gamma}{2} \log(q_1^2 + q_2^2) + \log\left(\frac{1}{2}(p_1^2 + p_2^2)\right) \quad (41)$$

using a scaled time. Numerical integration of this part requires very simple and fast evaluations and we neglect its cost in the results we present (we have solved this part using the S_{178} method, but for this problem similar results were obtained using the S_{96} method). We solve the separable system (40) using the RKN_{64} and the RKN_{116} methods.

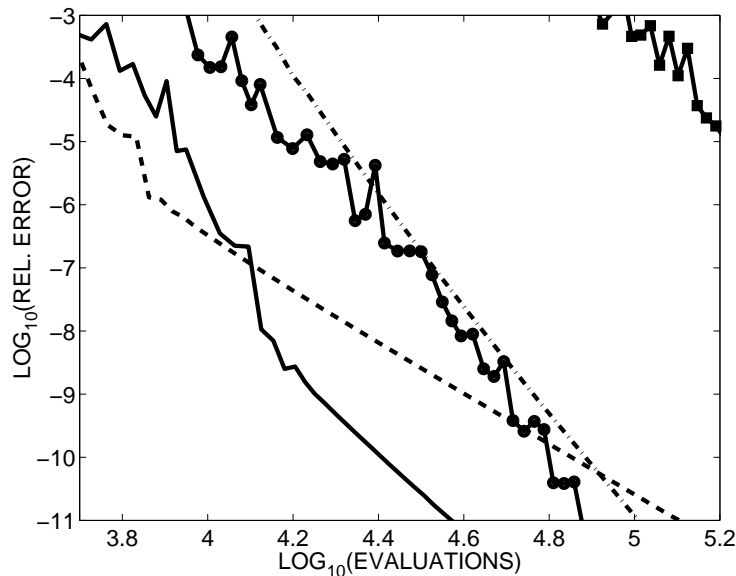


Fig. 4 Average error in energy in the numerical integration of (38) (for $\varepsilon = 10^{-3}$, $e = 0.8$ and integrated up to $t = 1000$). The results for the following schemes are shown: S_{178} with the Sundman transformation (dash-dotted line) and for the logarithmic Hamiltonian (42) (line with circles), the Poincaré transformation for the Hamiltonian (41) using the RKN methods of order four (dashed line) and of order six (solid line), and the sixth-order RKN method when no regularization is considered ($\gamma = 0$) (line with squares).

Finally, we consider the logarithmic method Mikkola and Tanikawa (1999); Preto and Tremaine (1999) corresponding to the integration of the Hamiltonian

$$K = \log \left(\frac{1}{2}(p_1^2 + p_2^2) + p^t \right) - \log \left(\frac{1}{r} - \frac{\varepsilon}{r^3} \right). \quad (42)$$

This is an efficient method for perturbed Kepler problems because it exactly solves the pure Kepler problem Preto and Tremaine (1999). Since the Hamiltonian has no kinetic energy quadratic in momenta, we integrate the system using S_{96} and S_{178} (we carried out numerical experiments of this method in the previous one-dimensional problem, which resulted in very low performance).

Fig. 4 shows the most relevant results: S_{178} with the Sundman transformation (dash-dotted line) and for the logarithmic Hamiltonian (42) (line with circles), the Poincaré transformation for the Hamiltonian (41) using the RKN methods of order four (dashed line) and of order six (solid line). As an illustration, we show the results of the sixth-order RKN method when no regularization is considered ($\gamma = 0$) (line with squares).

We have observed in numerical examples not reported here that both the Sundman and the Poincaré transformations exhibit very similar accuracies when used with the appropriate regularization function (and function $G(z)$ in the first case) and when they are integrated using the same splitting method. The main difference occurs when different splitting methods can be used with each formulation. We have not considered the computational cost of both choices since might be problem dependent. The Sundman transformation is more general and can be used

for solving other non Hamiltonian problems while the Poincaré transformation allows in some cases to use more efficient splitting methods, but is constrained to Hamiltonian systems.

The logarithmic Hamiltonian (42) can provide efficient algorithms for perturbed Kepler problems, but its performance with other problems is not so clear.

4.2.1 Adaptive methods for near-integrable systems

Finally, we analyse the performance of the Poincaré transformation for perturbed Hamiltonians while employing the monitor function given in (27). In particular, we consider

$$\bar{H} = \left(\frac{1}{2}(p_1^2 + p_2^2) - \frac{1}{r} + p^t \right)^\gamma - \left(-\frac{\varepsilon}{r^3} \right)^\gamma. \quad (43)$$

Here, $\frac{1}{2}(p_1^2 + p_2^2) - \frac{1}{r} + p^t$ is a positive function only if $-\frac{\varepsilon}{r^3}$ is a positive function. If $\varepsilon > 0$, the Hamiltonian to be integrated would be

$$\bar{H} = - \left(-\frac{1}{2}(p_1^2 + p_2^2) + \frac{1}{r} - p^t \right)^\gamma + \left(\frac{\varepsilon}{r^3} \right)^\gamma. \quad (44)$$

In the following we will only consider this problem with negative values of ε .

The Hamiltonian is separable into solvable parts. The case $\gamma = 1$ corresponds to the nonregularized case and has exactly the same complexity and computational cost as for different values of γ if one considers that the evolution of a Hamiltonian H_1 is the same as the evolution of $H_2 = F(H_1)$ with a scaled time $F'(H_1)$.

This splitting for nonregularised problems ($\gamma = 1$) is convenient for a small value of ε and low eccentricities, and this can be further improved by using splitting methods tailored for perturbed problems Laskar and Robutel (2001); McLachlan (1995a). We consider $\varepsilon = -10^{-3}$ and different values for the eccentricities (for the unperturbed problem), $e = 0.2$, $e = 0.5$ and $e = 0.8$. We use the following fourth-order splitting methods: S_{54} and M_{84} . Figure 5 shows the results obtained when no regularization is considered ($\gamma = 1$) (left figure). The convenience in using a splitting method tailored for perturbed problems is clear. We have repeated the experiment taking the regularization with $\gamma = 0.4$ (this is close to the optimal value we have observed for this problem and high eccentricities) (right figure). We observe that for $e > 0.2$ it is always more efficient to use regularization. Now, S_{54} shows similar or even superior performance than M_{84} . This is due to the fact that the regularization makes both parts relatively small and of similar size, and it is not advantageous to use methods tailored for perturbed problems. In the following, when this regularization is considered, we will only use S_{mn} methods.

Finally, we compare the performance of different S_{mn} splitting methods applied to (43) versus the RKN_{mn} methods applied to (40). The cost is very much problem dependent, and we measure here the number of evaluations in lieu of the cost (this value for the cost should be adjusted depending on the problem). Fig. 6 shows in the left panel the results obtained for the choices $e = 0.8$ and $\varepsilon = -10^{-3}$: solid lines correspond to the RKN_{64} and RKN_{116} methods for the Hamiltonian (40) and dashed lines correspond to the S_{54} , S_{96} and S_{178} methods applied to (43) with $\gamma = 0.4$. In this case the perturbation contributes strongly and the RKN methods exhibit the best performance. We have repeated the numerical experiment for the choices $e = 0.5$ and $\varepsilon = -10^{-5}$, which correspond to a moderate eccentricity with a

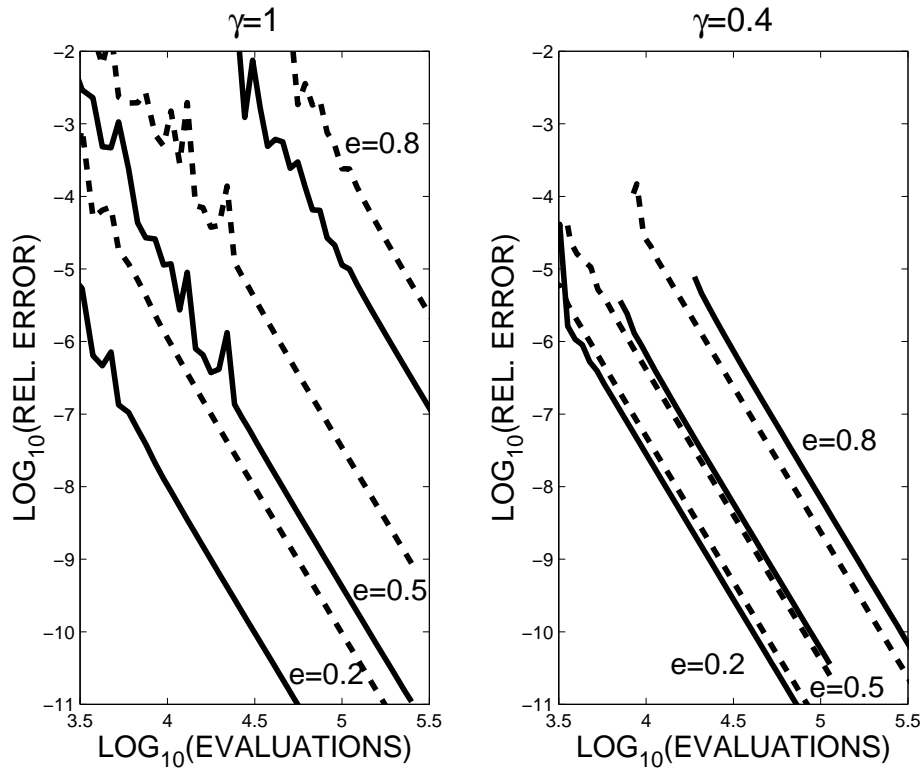


Fig. 5 Average error in energy in the numerical integration of (43) for $\varepsilon = -10^{-3}$, for different values of the eccentricity, e , and up to $t = 1000$. Two fourth-order splitting methods are used: S_{54} for general separable systems (dashed lines) and the (8,4) 5-stage BAB given in McLachlan (1995a) tailored for perturbed problems. The left figure corresponds to no regularization ($\gamma = 1$) and the right figure corresponds to the regularization with $\gamma = 0.4$.

very small perturbation (right panel). In this case, the methods for the perturbed problem with regularisation show the best performance. For illustration, we include the results for S_{178} when no regularisation is considered ($\gamma = 1$) (dotted line) (the results for the $M84$ method remains very close to the RKN_{116} method, and for clarity in the presentation it has not been shown in the figure).

From the numerical experiments we observe that both procedures for the Poincaré transformation exhibit good performance. The best choice is bound to depend on the problem. While the RKN methods applied to (40) need an efficient algorithm to solve the part which mixes coordinates and momenta, the splitting for the Hamiltonian (43) needs both parts to be positive definite. Were this not the case, one could have considered the Hamiltonian (28) which requires an efficient numerical integration of the Hamiltonian (29). This calls for further research.

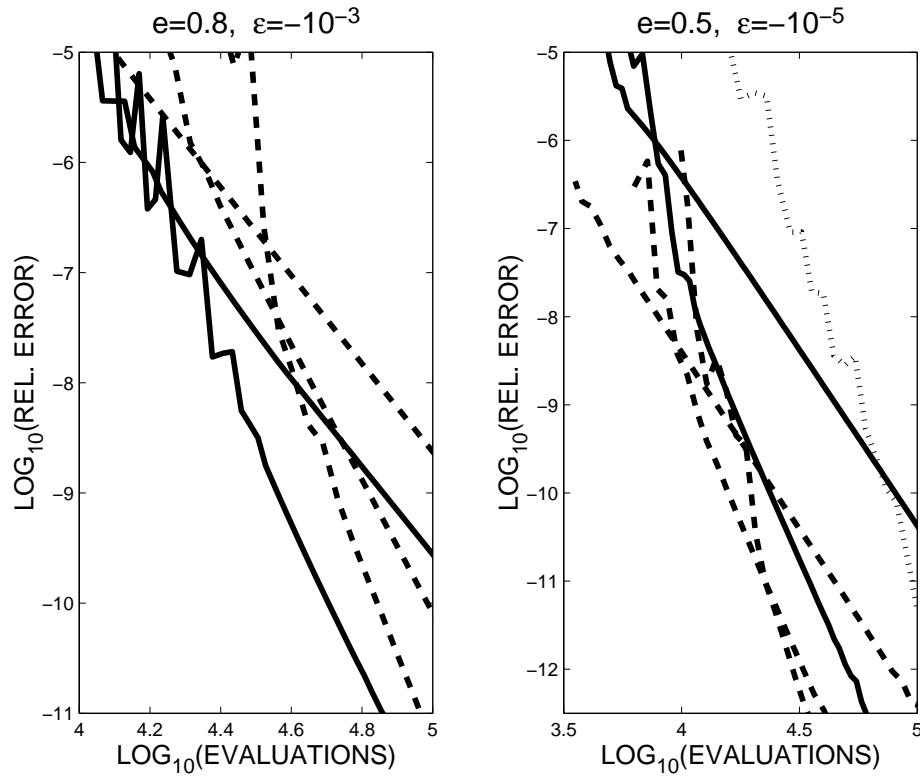


Fig. 6 Average error in energy in the numerical integration of (38) integrated using the S_{54} , S_{96} and S_{178} methods applied to (43) with $\gamma = 0.4$ (dashed lines), and the RKN_{64} and RKN_{116} methods applied to (40) with $\gamma = 3/2$ (solid lines). These methods can be distinguished by the slope of the curves. Left panel: corresponds to the choice $e = 0.8$ and $\varepsilon = -10^{-3}$. Right panel: corresponds to the choice $e = 0.5$ and $\varepsilon = -10^{-5}$. The results for S_{178} when no regularisation is considered ($\gamma = 1$) is also shown (dotted line).

4.3 The two-fixed-centres problem

We finally consider the two-dimensional two-fixed-centres problem

$$H = \frac{1}{2}(p_1^2 + p_2^2) - \frac{2\mu}{r_1} - \frac{2(1-\mu)}{r_2}, \quad (45)$$

with $r_1 = \sqrt{(q_1 - c)^2 + q_2^2}$, $r_2 = \sqrt{(q_1 + c)^2 + q_2^2}$. We take $\mu = 0.4$, $c = 1$ and initial conditions $q_1 = 1/2$, $q_2 = 0$, $p_1 = 0$, $p_2 = \sqrt{3}$ which has close approaches to one of the singularities (see Figure 7).

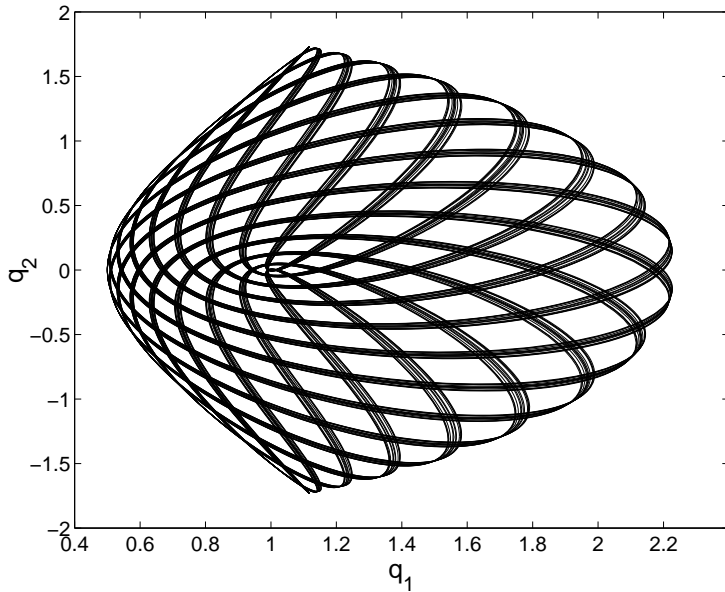


Fig. 7 Solution for the two-fixed-centres problem (45) for $t \in [0, 1000]$ and parameters given in the text .

For this problem we take the monitor function $g = r_1^\gamma r_2^\gamma$ for $\gamma = \frac{3}{2}$, and we take the Sundman transformation with $G(z) = 1/z$ and the splitting

$$\frac{d}{d\tau} \begin{Bmatrix} \mathbf{q} \\ \mathbf{p} \\ t \\ z \end{Bmatrix} = \underbrace{\begin{Bmatrix} \frac{1}{z}\mathbf{p} \\ z\mathbf{0} \\ 0 \\ 0 \end{Bmatrix}}_{\mathbf{f}_A} + \underbrace{\begin{Bmatrix} \mathbf{0} \\ \mathbf{0} \\ 0 \\ -\gamma \left(\frac{R_1}{r_1^2} + \frac{R_2}{r_2^2} \right) \end{Bmatrix}}_{\mathbf{f}_B} + \underbrace{\begin{Bmatrix} \mathbf{0} \\ -g\nabla V(\mathbf{q}) \\ \frac{1}{z} \\ 0 \end{Bmatrix}}_{\mathbf{f}_C} \quad (46)$$

with $R_1 = (q_1 - c)p_1 + q_2 p_2$, $R_2 = (q_1 + c)p_1 + q_2 p_2$. This corresponds, basically, to the split (14), as proposed in Mikkola and Aarseth (2002), but separated in three parts for simplicity.

We consider the S_{178} method as a composition of the symmetric second order (11) and we take a fictive time step such that the final real time, $t = 1000$, is reached with approximately 50000 evaluations of the potential, and measure the error in energy along the time integration.

We repeated the numerical experiment replacing the term $-g\nabla V(\mathbf{q})$ in f_C , which is not the gradient of a potential, by $-(\nabla V(\mathbf{q}))/z$, which preserves symplecticity. The results are shown in Fig. 8 where the highest performance of the symplectic scheme is clear. As previously mentioned, this deserves further investigation.

If one considers the Poincaré transformation then RKN symplectic methods can be used if the Hamiltonian $K_1 = r_1^\gamma r_2^\gamma (p_1^2 + p_2^2)/2$ is exactly solved, or numerically solved up to high accuracy. For this problem it is clear that we can not use a

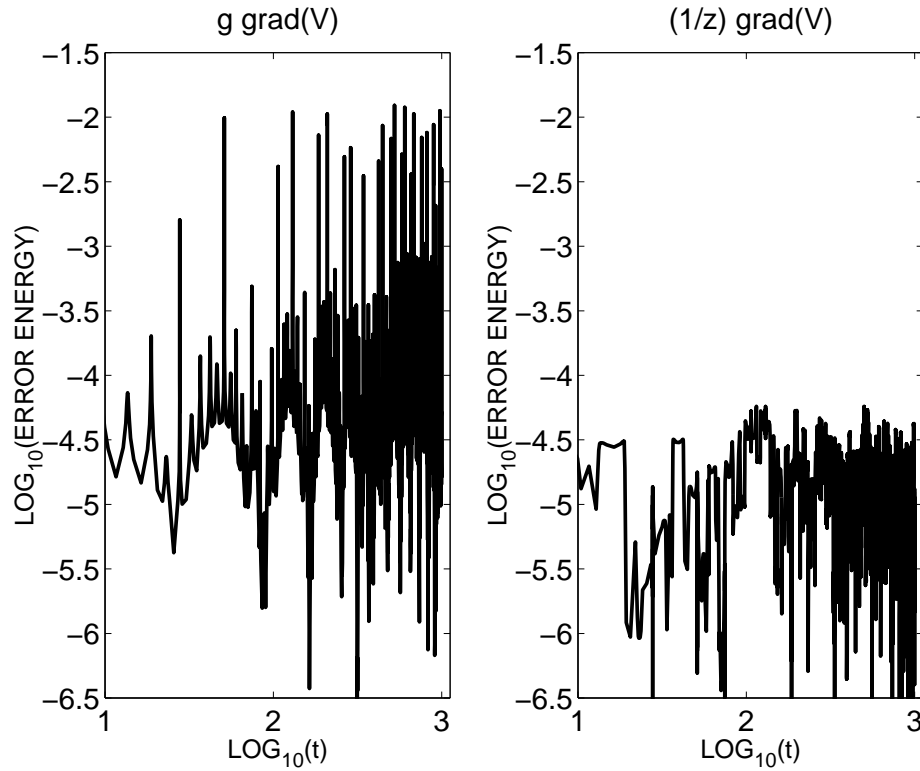


Fig. 8 Error in energy along the time integration for the two-fixed-centres problem (45) for the split (46) (left panel) and when the term $-gV(\mathbf{q})$ in f_C is replaced by $-(\nabla V(\mathbf{q}))/z$ (right panel) .

canonical transformation to solve it, but the logarithmic method can be used very easily to high accuracy and low computational cost.

5 Conclusions

We have considered the Sundman and the Poincaré transformation for the numerical integration of separable Hamiltonian systems evolving at different time scales. We have considered both transformation in their general form. This allowed us to obtain, in a simple form, most algorithms proposed in the recent literature as particular cases. We have also constructed new highly efficient methods, displaying their best performance when a high accuracy is desired.

The numerical experiments suggest that, in general, both the Sundman and the Poincaré transformations provide similar accuracy if an appropriate regularization function is chosen (which can differ in each case) and the same splitting method is used in both cases. The main difference remains in the fact that the Poincaré transformation allows, in some cases, to retain the structure of the original Hamiltonian (e.g. quadratic in momenta or near-integrable) and one can use splitting methods tailored for these problems. This requires the numerical integration of

new Hamiltonian functions with a relatively simple and very particular structure whose efficient integration allows to end up with highly efficient algorithms. The Sundman transformation is, however, more general and can be easily used on non Hamiltonian systems.

The results presented in this work easily extend to time-dependent potential functions $V(\mathbf{q}, t)$ by considering the time as a new coordinate as well as to other separable Hamiltonian functions.

References

- Blanes S, Budd CJ (2004) High order symplectic integrators for perturbed hamiltonian systems. *Celestial Mechanics and Dynamical Astronomy* 89:383–405
- Blanes S, Budd CJ (2005) Adaptive geometric integrators for hamiltonian problems with approximate scale invariance. *SIAM J Sci Comput* 26:1089–1113
- Blanes S, Moan PC (2002) Practical symplectic partitioned runge–kutta and runge–kutta–nyström methods. *J Comp Appl Math* 142:313–330
- Blanes S, Casas F, Ros J (1999) Extrapolation of symplectic integrators. *Celestial Mechanics and Dynamical Astronomy* 75:149–161
- Blanes S, Casas F, Murua A (2008) Splitting and composition methods in the numerical integration of differential equations. *Bol Soc Esp Mat Apl* 45:89–145
- Bond SD, Leimkuhler B (1998) Time-transformations for reversible variable step-size integration. *Numerical Algorithms* 19:55–71
- Budd CJ, Leimkuhler B, Piggott MD (2001) Scaling invariance and adaptivity. *Appl Numer Math* 39:261–288
- Calvo MP, Sanz-Serna JM (1993) The development of variable-step symplectic integrators, with applications to the two-body problem. *SIAM J Sci Comput* 14:936–952
- Calvo MP, Sanz-Serna JM, López-Marcos MA (1998) Variable step implementations of geometric integrators. *Appl Numer Math* 28:1–16
- Chan RPK, Murua A (2000) Extrapolation of symplectic methods for hamiltonian problems. *Appl Numer Math* 34:189–205
- Creutz M, Gocksch A (1989) Higher-order hybrid monte carlo algorithms. *Phys Rev Lett* 63:9–12
- Gladman B, Duncan M, Candy J (1991) Symplectic integrators for long-term integrations in celestial mechanics. *Celestial Mechanics* 52:221–240
- Hairer E (1997) Variable time step integration with symplectic methods. *Appl Numer Math* 25:219–227
- Hairer E, Söderlind G (2005) Explicit, time reversible, adaptive stepsize control. *SIAM J Sci Comput* 26:1838–1851
- Hairer E, Lubich C, Wanner G (2006) *Geometric Numerical Integration. Structure-Preserving Algorithms for Ordinary Differential Equations*, vol 31, Second edn. Springer-Verlag
- Holder T, Leimkuhler B, Reich S (2001) Explicit variable step-size and time-reversible integration. *Appl Numer Math* 39:367–377
- Huang W, Leimkuhler B (1997) The adaptive verlet method. *SIAM J Sci Comput* 18:239–256
- Iserles A (2008) *A First Course in the Numerical Analysis of Differential Equations*, Second edn. Cambridge University Press

- Kinoshita H, Yoshida H, Nakai H (1991) Symplectic integrators and their application to dynamical astronomy. *Celestial Mechanics and Dynamical Astronomy* 50:59–71
- Laskar J, Robutel P (2001) High order symplectic integrators for perturbed hamiltonian systems. *Celestial Mechanics and Dynamical Astronomy* 80:39–62
- Leimkuhler B, Reich S (2004) *Simulating Hamiltonian Dynamics*. Cambridge University Press
- McLachlan RI (1995a) Composition methods in the presence of small parameters. *BIT Numerical Mathematics* 35:258–268
- McLachlan RI (1995b) On the numerical integration of ordinary differential equations by symmetric composition methods. *SIAM J Sci Comput* 16(1):151–168
- McLachlan RI, Quispel RGW (2002) Splitting methods. *Acta Numerica* 11:341–434
- McLachlan RI, Quispel RGW (2006) Geometric integrators for odes. *J Phys A: Math Gen* 39:5251–5285
- Mikkola S (1997) Practical symplectic methods with time transformation for the few-body problem. *Celestial Mechanics and Dynamical Astronomy* 67:145–165
- Mikkola S, Aarseth S (2002) A time-transformed leapfrog scheme. *Celestial Mechanics and Dynamical Astronomy* 84:343–354
- Mikkola S, Tanikawa K (1999) Explicit symplectic algorithms for time-transformed hamiltonians. *Celestial Mechanics and Dynamical Astronomy* 74:287–295
- Preto M, Tremaine S (1999) A class of symplectic integrators with adaptive time step for separable hamiltonian systems. *Celestial Mechanics and Dynamical Astronomy* 118:2532–2541
- Sanz-Serna JM, Calvo MP (1994) *Numerical Hamiltonian Problems*. Chapman and Hall
- Skeel R (1993) Variable step size destabilizes the störmer/leapfrog/verlet method. *BIT Numerical Mathematics* 33:172–175
- Sophoniu M, Spaletta G (2005) Derivation of symmetric composition constants for symmetric integrators. *Optimization Methods Software* 20:597–613
- Stiefel EL, Scheifel G (1971) *Linear and regular celestial mechanics*. Springer, Berlin
- Suzuki M (1990) Fractal decomposition of exponential operators with applications to many-body theories and monte carlo simulations. *Physics Letters A* 146(6):319 – 323
- Wisdom J, Holman M (1991) Symplectic maps for the n-body problem. *Astronomical Journal* 102:1528–1538
- Yoshida H (1990) Construction of higher order symplectic integrators. *Physics Letters A* 150(5-7):262 – 268